233 (2024) 212470

Contents lists available at ScienceDirect

Geoenergy Science and Engineering

journal homepage: www.sciencedirect.com/journal/geoenergy-science-and-engineering

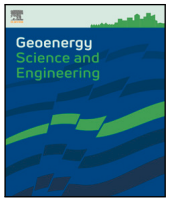

Implementation of a Reduced Order Model for rotating seal annular leakage flow inside a centrifugal pump

Johannes Petrus van der Walt, Jan-Hendrik Kruger *, Charl Gabriël du Toit

School of Mechanical Engineering, North-West University, 11 Hoffman Street, Potchefstroom, 2531, North-West Province, South Africa

ARTICLE INFO

Keywords:
Suction wear ring
Annular leakage flow
CFD analysis
Ansys CFX CEL
Reduced Order Model (ROM)
Centrifugal pump annular seal

ABSTRACT

Sustainability and net zero emissions targets drive the importance of turbomachinery design, optimisation, and efficient operation in modern geoenergy systems. To further enable integration of advanced large-scale technologies, accurate and resource-efficient simulations of complex equipment and systems need to be completed readily. An approach to simulate internal leakage flows of centrifugal pumps is presented, an important factor that influences equipment operation efficiency.

One significant challenge when internal leakage flow is investigated is achieving sufficient simulation detail in the flow regions separating rotating and stationary components where close-running clearances are present. Computational fluid dynamics (CFD) meshes typically require excessively fine resolutions of node points in these situations for accuracy. For example, the typical annular suction wear ring clearance ranges between 0.1–0.5 mm, whilst impeller diameters and other geometric properties have length scales from 600–1200 mm or even larger.

A reduced order model (ROM) of an annular seal configuration was developed that allows for analytical calculation of the leakage flow by implementing user scripting in the CFD solver setup. The ROM implementation has a low symbol count and does not require any type of logic and/or recursive and iterative functionality. Thus, fine and resource-intensive meshing can be robustly eliminated and replaced by a sufficiently detailed ROM that contributes leakage flow effects to the overall simulation.

Leakage flow through the suction wear ring of a high differential head (ΔH), high flow rate, double suction centrifugal pump with water as working fluid was used as a case study for ROM development. The calibrated model was verified against a commercial fluid dynamics software package and achieved a level of precision of 2.4% with $\sigma = 0.0118$ in a wide operating range of $10\,\text{m} \leqslant \Delta H \leqslant 350\,\text{m}$ and fluid temperature (T) of $283.15\,\text{K} \leqslant T \leqslant 353.15\,\text{K}$.

The leakage flow calculated by the ROM was proven to be accurate and therefore capable of accounting for a range of pressure heads, incorporating surface roughness effects and temperature variations, and adaptable for various fluids. Guidance for the implementation of the ROM in the Ansys CFX solver environment is also provided to aid future work.

1. Introduction

The design and operation efficiency of turbomachinery play a pivotal role in the advancement of modern geoenergy systems, aligning with the imperatives for sustainability and net zero emissions. By integrating simulation technologies of different scales, resource-efficient modelling approaches can target leakage flows in centrifugal pumps, a critical factor that influences equipment performance and energy system optimisation. In the turbomachine environment, the annular seal can be described as a small fluid-filled annular clearance between a stationary outer cylinder and a rotating inner cylinder with a fixed axial length. The seal configuration can be of various designs, including but not limited to: cylindrical, serrated, labyrinth, grooved, and stepped.

Annular seals allow centrifugal pumps to operate in a satisfactory manner. The annular seal configuration is present at all wearing surfaces between the rotor and stator interfaces, where a seal is required between two individual high- and low-pressure chambers. Some examples where effective sealing is required are: impeller wear rings, balance pistons/drums, and neck bush interfaces in multistage rotor arrangements.

* Corresponding author.
E-mail addresses: jp.vanderwalt@tutanota.com (J.P. van der Walt), janhendrik.kruger@nwu.ac.za (J.-H. Kruger), cgdt@mtechindustrial.com (C.G. du Toit).
URL: https://engineering.nwu.ac.za/mechanical-engineering/staff (J.-H. Kruger).

https://doi.org/10.1016/j.geoen.2023.212470
Received 11 May 2023; Received in revised form 2 October 2023; Accepted 5 November 2023
Available online 7 November 2023

Nomenclature

API	American Petroleum Institute
API	Application Programming Interface
BEP	Best Efficiency Point
CEL	CFX Expression Language
CFD	Computational Fluid Dynamics
NPSHR	Net Positive Suction Head Required [m]
OD	Outside Diameter [m]
PLC	Programmable Logic Controller
ROM	Reduced Order Model
π	Circumference/diameter of circle 3.14...
g	Gravitational acceleration 9.81 m/s^2
ΔH	Static head difference across annulus [m]
η	Operating efficiency [%]
λ	Annular friction coefficient [−]
μ	Dynamic viscosity of fluid [N s/m^2]
ν	Kinematic viscosity of fluid [m^2/s]
ρ	Density of fluid [kg/m^3]
σ	Standard deviation of a data set [−]
ϵ	Equivalent sand surface roughness [m]
ζ_A	Exit pressure loss coefficient [−]
ζ_{EA}	Total hydraulic pressure loss coefficient [−]
ζ_E	Entrance pressure loss coefficient [−]
A	Roughness compensation factor [−]
$a...z$	Polynomial regression coefficients [−]
C, K	Polynomial regression constants [−]
c_{ax}	Axial velocity in annulus [m/s]
d_{imp}	OD of impeller [m]
d_{sp}	OD of rotating inner cylinder of annulus [m]
H	Head delivered per pump stage [m]
i, j, y	Numerical list counters (super-, subscripts) [−]
L_{sp}	Annulus axial length [m]
n	Rotational speed of the impeller [RPM]
P	Electrical power [kW]
p	Absolute pressure of fluid [Pa(a)]
Q	Volumetric flow rate of pump [m^3/s]
Q_{sp}	Annular leakage volumetric flow rate [m^3/s]
r_{sp}	Outer radius for d_{sp} [m]
Re	Axial Reynolds number in annulus [−]
Re_u	Reynolds number for circumferential flow [−]
s	Radial annular clearance [m]
T	Temperature of fluid [K]
u_{sp}	Wear ring tip velocity [m/s]

It is of paramount importance for the pump designer (and user) to understand the impact of annular seal clearance and the variation of such dimensions on the operation and performance of centrifugal pumps in general. The magnitude of the internal leakage flow rate is directly related — and very sensitive — to the annular seal clearance. When an increase in annular seal clearance is observed, a noticeable influence on the total flow rate through the impeller coupled with a shift of the operating point to the right of the performance curve (and a subsequent detrimental NPSHR shift) has been highlighted in various texts including Volk (2013), Bloch (2011) and Yedidiah (1996). Furthermore, Gülich (2014) states that the amount of observable annular leakage (Q_{sp}) increases proportionately to an increase in annular clearance (s) by $Q_{sp} \propto s^{1.5}$, with a more pronounced effect in the case of designs of low specific speed pumps.

Although some industry standards such as API STD 610 (American Petroleum Institute, 2011) provide guidance on recommended annular seal clearances, most original equipment manufacturers have their own design methodologies and clearance requirements for annular seal arrangements. Usually, the specified clearances are not solely specified to account for an optimal internal leakage restriction, but also to counteract various mechanical concerns, such as: shaft deflection and rotordynamic stability, materials prone to galling when in service, etc. The calculation of internal leakage through rotating annular seals is thus a primary concern for pump designers to enable accurate performance prediction of new and revised machine configurations.

Easily accessible computing resources have resulted in the increasing utilisation of CFD to aid the pump designer in determining accurate performance parameters rapidly. However, the modelling of rotating annular seals is a major difficulty in full pump 3D CFD applications due to excessive mesh density requirements in the vicinity of the annular seals, as mentioned by Liebner et al. (2016) and Páscoa et al. (2010), especially when more than one annular seal is modelled, as in the case of multistage pumps. In addition, obtaining convergent solutions becomes even more challenging due to the extreme difference in length scales between cells in the annular region of the seal and the remainder of the flow domain. It has been found by Van der Walt (2021) that this could lead to divergent and unstable numerical behaviour, particularly with transient simulations under high differential pressure flow conditions.

In order to aid in numerically robust and less computationally intensive simulations, an alternative method is therefore required to calculate annular leakage flows — in real time — in large, detailed 3D CFD models.

Using the user-coding within general CFD software, functionality can be extended to address specialised flow phenomena, such as annular leakage flow, with more appropriate models than those provided in the main codebase. Since the application of user-coding is very case-specific, 3D CFD submodels are therefore not generally provided to address annular leakage flow.

This paper presents a novel approach to accurately model the leakage flow in short annular seals by means of a reduced-order model (ROM). The implementation was derived from an existing iterative analytic method but was adapted not to require any type of logic and/or recursive and iterative functionality, which improves numerical efficiency and stability. The ROM model was verified against a model from the Flownex (Flownex International, 2023) commercial CFD software and subsequently applied as an expression in Ansys (Ansys, Inc., 2023) CFX Expression Language.

Section 2 presents the theoretical model used in the development of the ROM described in Section 3. The verification process and results are given in Section 4 with an example implementation in Ansys CEL described in Section 5. Section 6 concludes.

2. Theoretical model

The predictable geometry of most annular seal types currently used in turbomachinery design and construction, along with computationally expensive CFD modelling requirements and sufficient available research related to flow field characteristics, make internal leakage through annular seals an attractive candidate for ROM construction. Before undertaking any ROM development actions, a reliable theoretical model should be identified to model the system of concern. The selected model and its implementation are explained in the following section.

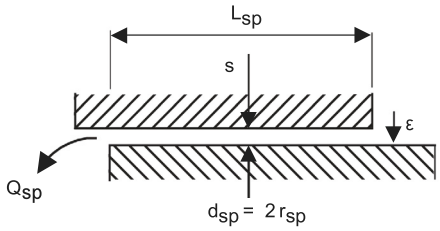

Fig. 1. Geometry of single stage annular seal (Gülich, 2014).

2.1. Modelling methodology

In order to accurately describe leakage flow through an annular seal, certain key variables must be included in the evaluation. These are illustrated in Fig. 1 and include: The inlet and outlet geometry, rotating inner cylinder of the annulus (d_{sp}), the length of the seal (L_{sp}), the annular radial clearance of the seal (s) and the roughness (ε) of the wetted surface area of the seal. The surface effects in this case cannot be ignored due to the large ratio of surface roughness to flow field height.

The model selected for the calculation of the volumetric leakage flow rate was developed by Gülich (2014). The accuracy of the predicted values of the model was verified through comparison with the results obtained using a commercial fluid dynamics software package.

In order to calculate the volumetric flow rate through a rotating annulus, a good understanding of the fluid properties is important. Kinematic viscosity (ν) is the most important fluid parameter in the current method and is described by $\nu = \mu/\rho$ (Munson et al., 2013). It is important to note that since this value will change with temperature and pressure, adequate compensation should be made to ensure the accuracy of the model. The model is only valid for fully turbulent flow in the annulus.

$$Q_{sp} = \pi d_{sp} s c_{ax} \tag{1}$$

As shown in Eq. (1), the volumetric leakage flow rate (Q_{sp}) is directly dependent on the outer diameter (OD) of the rotating inner cylindrical surface (d_{sp}), the measured radial clearance between the rotating and stationary surfaces (s), and the axial flow velocity of the fluid in the annulus (c_{ax}).

The formulation for the calculation of c_{ax} is given in Eq. (2). Note the further dependency on various variables, including the difference in head observed across the annulus (ΔH) and the annular friction coefficient (λ). Although it is possible to approximate ΔH analytically, it is not recommended due to the fact that this variable can be calculated and continuously updated by referencing static pressure values extracted from the main flow field generated by the CFD simulation runtime.

$$c_{ax} = \sqrt{\frac{2g\Delta H}{\zeta_{EA} + \lambda \frac{L_{sp}}{2s}}} \tag{2}$$

$$\zeta_{EA} = \zeta_E + \zeta_A \tag{3}$$

In Eq. (3) the total hydraulic pressure loss coefficient (ζ_{EA}) of the annulus consists of the inlet pressure loss coefficient (ζ_E) and the outlet pressure loss coefficient (ζ_A) and were approximated using the methodology presented in Table 1.4 from Gülich (2014); however, these values can also be approximated using alternative methods described in authoritative texts on fluid mechanics such as Rennels and Hudson (2012). Inlet and outlet loss coefficients were calculated as those for a sudden contraction and a sudden expansion, with rounded edges and without a backwall arrangement. These coefficients can have an unexpectedly large impact on the total flow rate computed through the annulus, and care should be taken during the design of such devices.

The hydraulic friction loss coefficient (λ) in Eq. (4) ensures that the friction caused by the roughness of the surface in the axial direction is taken into account while simultaneously compensating for the rotational effect experienced by the fluid as it passes through the rotating annular geometry. The addition of the effect of surface roughness is extremely beneficial for the analyst, and this is one of the main benefits of using the current theoretical model.

$$\lambda = \underbrace{\left[1 + 0.19\left(\frac{Re_u}{Re}\right)^2\right]^{0.375}}_{\text{Influence of rotation}} \underbrace{\left[\frac{0.31}{\log\left(A + \frac{6.5}{Re}\right)^2}\right]}_{\text{Friction coefficient}} \tag{4}$$

However, the model is highly implicit, since the Eqs. (2), (4), and (8) are interdependent. Re cannot be computed without taking into account the other equations mentioned.

The roughness compensation factor (A) is given by

$$A = 0.135\frac{\varepsilon}{s}, \tag{5}$$

with the wear ring tip velocity (u_{sp}) calculated as

$$u_{sp} = \frac{\pi d_{sp} n}{60}. \tag{6}$$

The Reynolds number (Re_u) at the OD of wear ring for circumferential flow is given by

$$Re_u = \frac{2 s u_{sp}}{\nu}, \tag{7}$$

with the axial Reynolds number (Re) of flow in the annulus:

$$Re = \frac{2 s c_{ax}}{\nu}. \tag{8}$$

To determine Re, Eq. (4) is substituted in (2); Eq. (8) is rewritten to isolate c_{ax} and then equated with Eq. (2). The mentioned manipulations produce Eq. (9).

$$\frac{\nu Re}{2s} = \sqrt{\frac{2g\Delta H}{\zeta_{EA} + \lambda \frac{L_{sp}}{2s}}} \tag{9}$$

Although highly implicit, the reduced and simplified Eq. (9) allows the implementation of numerical root finding algorithms, as the only truly unknown variable is Re. The root-finding algorithm implemented in the study was the secant method, as detailed in Bradie (2006). After determining the axial Reynolds number, Re, a simple substitution can be implemented to find the remaining dependent variables and finally Q_{sp}.

The ROM implementation presented in Section 3, was derived from the implicit method described above. If implemented correctly, no iterative or recursive solving methods are required to solve the ROM. The explicit nature of the mathematical formulation ensures the numerical efficiency and local stability of the seal region in the overall CFD simulation.

3. Reduced order model (ROM)

The main purpose of a ROM is to substitute a complex system of equations/methods/models, often encompassing iterative or numerical methods, with a simpler — but still mathematically equivalent — analytic equation (or system of equations) that can be evaluated rapidly and implemented on demand. The effective implementation of ROMs in complex computational simulations (e.g. CFD analyses) can dramatically reduce grid resolution and improve mesh quality metrics in problematic portions of the domain, thereby ensuring better numerical stability and reducing solver run-times without sacrificing solution accuracy.

In order to construct a ROM for use in general engineering applications, a large amount of reliable data is required to be obtained to use as input for the construction of the mathematical model. The data required relate to the system being evaluated and the dependence of the particular system on variables such as temperature, pressure, etc.

The modelling approach presented in this paper originated from an idea of calculating all possible outcomes from a particular circumstance (keeping certain conditions fixed) and fitting a model to those points. The approach enables robust interpolation without iteration between the calculated points, based on a single variable input (naturally, a system of equations should be built for additional variable dependencies). The underlying physics of the annular leakage flow is referenced in Section 2 and was used to inform the ROM methodology that follows.

3.1. Choice of regression model

The choice of regression approach for the 1D ROM is crucial since it ultimately determines the accuracy and numerical robustness of the modelling strategy, especially when it is incorporated into a more detailed and complex 3D CFD simulation. To represent the values from the Gülich theoretical model, Kriging, rational functions and Fourier transforms were considered as options before polynomial functions was finally chosen as the regression technique.

3.1.1. Original motivation

The ROM procedure was adapted from a method the first author had originally developed to streamline in-house digital twins of complex flow systems within the petrochemical environment. The twin models were hard-coded into the plant's information system (data logging system for process monitoring) where the user-programmed calculation routines were curbed by symbol count and barred any type of logic and/or recursive and iterative functionality. Subsequently, the need arose to reduce complete equipment operating characteristics (turbo-compressors, turbines, multistage centrifugal pumps, etc.) into a simple expression, or a couple of intertwining simple expressions. Advantageously, this enabled explicit calculations to be performed without the need for iteration and resolved any potential mathematical difficulties that would crash the PLC (i.e. infinite loops or mathematical principle errors).

3.1.2. Alternative modelling options

Kriging regression (also known as Gaussian process regression) can be considered an iterative process (Krige, 1951). The process involves a feedback loop between the data and the chosen curve fit model (be it linear or more complex). The Kriging process itself involves an iterative step where weightings are computed for each neighbouring data point and the predicted value arising from the regression model is updated based on the weighting of the evaluated points. However, due to the fact that the scatter in the values of the mathematical model in Section 2 is essentially non-existent, and a very close polynomial fit is possible, the authors did not see any need for this type of regression analysis to be applied.

Using rational functions can be a forward approach, but due to the operational desire of keeping the ROM model brief, this method was also not considered. A polynomial function fits the calculated values from the mathematical model almost perfectly, so again, using a method such as the rational function approach would not add much value as there is almost no scatter in the theoretical values.

Fourier series analysis would be useful if there were noisy data which required a Fourier transform to be completed — additionally, the Fourier series is a sum of sine and cosine functions which introduces wiggles into the processed data (unless a sufficient number of terms are present to "iron out" the wiggles to an acceptable amplitude). In order to keep the model as concise as possible, the Fourier series was also not used as there is no need to adapt the ROM's compositional terms on the fly.

Table 1
Dependency of ROM variables.

Variable	Type	Dependency
Inputs		
s	Independent	Fixed geometry
d_{sp}	Independent	Fixed geometry
ΔH	Dependent	Extracted from CFD
Output		
Q_{sp}	Dependent	$c_{ax} \rightarrow Re \rightarrow \nu \rightarrow T, p$

3.1.3. Rationale for polynomial regression

Polynomial regression offers several advantages when used as a data regression strategy:

1. Due to the fact that the generated values from the theoretical model are exact and no scatter is reported, a polynomial curve fit through these values is possible and yields very accurate results without the need to perform complex curve fitting algorithms to increase accuracy.
2. To remove any additional/inherent implicit mathematics from the model, a marching-style regression is required.
3. The existing model can be easily modified to include annuli of various dimensions — without changing the structure of the ROM (this furthermore creates the possibility of developing a user API for general use).
4. It is straightforward to develop a polynomial model that solves very quickly without the risk of numerical instability or mathematical errors.
5. Regression can be applied only when one variable is independent (e.g. ΔH) and the dependent variables (in this case only T) are "stacked" and then interpolated in a 3D manner on the x- and z-axis. The polynomial curve fit model was proven to be accurate for the current application — implementation of alternative interpolation schemes could potentially impact calculation efficiency and accuracy in a negative manner.

3.2. Variable dependency

In order to construct an accurate ROM, it is important to determine which physical parameters will influence the system and how one will effectively account for these parameters. The first step is to determine the variable dependency of the theoretical model described in Section 2.

From Table 1, most variables related to the geometry of the installation of the annular seal are independent (that is, d_{sp}, s, ϵ, L_{sp}, etc.), while the parameters related to the flow and state of the fluid are dependent. It is notable that the leakage flow rate (Q_{sp}) is completely dependent on the axial Reynolds number (Re), while Re is, in turn, dependent on the kinematic viscosity of the fluid (ν), which is directly dependent on the fluid temperature (T) and pressure (p).

The differential head observed across the annular seal arrangement, ΔH, is unknown and will therefore have to be calculated and provided as input to the ROM. For the final dependent variable, the ROM is thus dependent on the main numerical model ("master") of the pump being simulated. In the workflow described here, the differential head is thus calculated using the CFX Expression Language (CEL) functions within Ansys CFX during the solution process.

3.3. Generation of theoretical base values

In order to construct a representative ROM, sufficient values relating the theoretical model to the physical system at different operating points are required to enable ROM setup.

Table 2 shows a structured approach to value generation; with a fixed geometry (annular inlet and outlet geometry, surface roughness ϵ, diameters, etc.), the Gülich model as described in Section 2 was

Table 2
Theoretical values representing the relationship between Q_{sp} and ΔH as a function of T for fixed geometry and roughness.

	T_0	T_1	T_2	…	T_i
ΔH_0	$Q_{sp0,0}$	$Q_{sp0,1}$	$Q_{sp0,2}$	…	$Q_{sp0,i}$
ΔH_1	$Q_{sp1,0}$	$Q_{sp1,1}$	$Q_{sp1,2}$	…	$Q_{sp1,i}$
ΔH_2	$Q_{sp2,0}$	$Q_{sp2,1}$	$Q_{sp2,2}$	…	$Q_{sp2,i}$
⋮	⋮	⋮	⋮		⋮
ΔH_j	$Q_{spj,0}$	$Q_{spj,1}$	$Q_{spj,2}$	…	$Q_{spj,i}$

Table 3
Polynomial regression applied per ΔH to describe Q_{sp} as a function of T.

ΔH_0	$x_0T^y + \ldots + b_0T^2 + a_0T + C_0 = Q_{sp0}$
ΔH_1	$x_1T^y + \ldots + b_1T^2 + a_1T + C_1 = Q_{sp1}$
ΔH_2	$x_2T^y + \ldots + b_2T^2 + a_2T + C_2 = Q_{sp2}$
⋮	⋮
ΔH_j	$x_jT^y + \ldots + b_jT^2 + a_jT + C_j = Q_{spj}$

Table 4
Polynomial regression of values in Table 3 to find polynomial coefficients for C as a function of ΔH.

ΔH_0	$z_0{\Delta H_0}^y + \ldots + r_0{\Delta H_0}^2 + q_0\Delta H_0 + K_0 =$	C_0
ΔH_1	$z_0{\Delta H_1}^y + \ldots + r_0{\Delta H_1}^2 + q_0\Delta H_1 + K_0 =$	C_1
ΔH_2	$z_0{\Delta H_2}^y + \ldots + r_0{\Delta H_2}^2 + q_0\Delta H_2 + K_0 =$	C_2
⋮	⋮	
ΔH_j	$z_0{\Delta H_j}^y + \ldots + r_0{\Delta H_j}^2 + q_0\Delta H_j + K_0 =$	C_j

solved for a range of expected ΔH and T values. After experimentation with liquid water over the range of values, it could be stated that p has a negligible influence on ν across the operating range expected in general turbomachinery applications and can be safely omitted from ROM construction.

3.4. Polynomial regression steps

The values generated in Table 2 should be made accessible by means of a number of regression steps, to ultimately find an expression for Q_{sp} as a function of the annular ΔH and fluid temperature (T).

3.4.1. Obtain leakage flow as function of differential head and temperature

Regression should be performed per row; thus, for each fixed value ΔH_j, the value of Q_{spj} as a function of T was determined.

Table 3 describes the intended regression steps and is represented by polynomial equations. Note that the regression formulae should be of the same type and order for every row (that is, per ΔH_j), and the format should be adapted to a scheme that best represents the values.

After the regression analysis is complete, Q_{spj} can be easily computed at any T (interpolated within the model range) with a single equation that corresponds to the specified ΔH_j.

3.4.2. Determine polynomial coefficients as a function of differential head

In order to enable greater flexibility in the regression functions and to condense the magnitude of the required equations, the sensitivity of the model to a range of ΔH had to be incorporated. Regression of individual polynomial coefficients was performed as a function of ΔH — of which the equation system for $C(\Delta H)$ is shown in Table 4.

Similarly, the process is repeated for the additional coefficients required, as described in Table 5. However, in this step the order and type of the generated regression equations need not all be similar in form and order.

Table 5
Polynomial regression of values in Tables 3 and 4 to find polynomial coefficients as a function of ΔH.

$z_0\Delta H^y + \ldots + r_0\Delta H^2 + q_0\Delta H + K_0 =$	$C(\Delta H)$
$z_1\Delta H^y + \ldots + r_1\Delta H^2 + q_1\Delta H + K_1 =$	$a(\Delta H)$
$z_2\Delta H^y + \ldots + r_2\Delta H^2 + q_2\Delta H + K_2 =$	$b(\Delta H)$
⋮	
$z_i\Delta H^y + \ldots + r_i\Delta H^2 + q_i\Delta H + K_i =$	$x(\Delta H)$

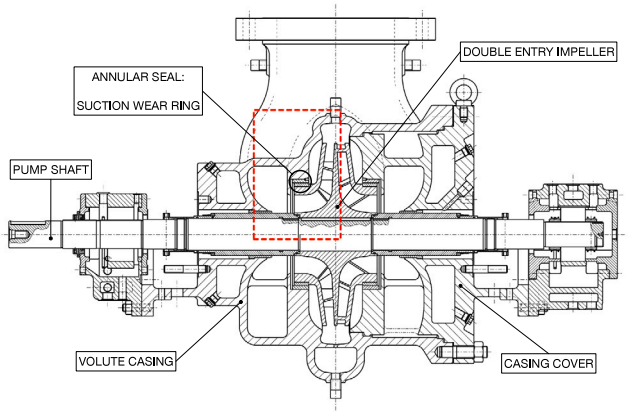

Fig. 2. Cross sectional drawing of subject pump, with part descriptions (Red dashed line area is detailed in Fig. 4).
Source: Adapted from Van der Walt (2021).

3.5. Final form of ROM

In order to combine the equation systems generated in Tables 3–5 into a single polynomial function, the functions that represent the polynomial coefficients were incorporated into the form of the original regression function in Table 3.

$$x(\Delta H)T^y + \cdots \\ \ldots + b(\Delta H)T^2 + a(\Delta H)T + C(\Delta H) = Q_{sp} \tag{10}$$

Eq. (10) then gives the final form of the ROM. This equation is a function of T and ΔH over the entire range of base model values. The annular leakage flow, Q_{sp} can therefore be predicted analytically with this single equation — along with its constituent coefficients — that can be programmed into a numerical solver environment.

4. Verification and calibration

4.1. Case study - double suction centrifugal pump

To demonstrate the preparation of the annular seal ROM for CFD analysis, the internal leakage generated by the suction wear ring of the double suction centrifugal pump in Fig. 2 is presented as a case study. The general layout of the impeller and volute is shown in Fig. 3.

The detailed location of the suction wear ring and the relevant flow regions with the ROM inlet and outlet boundaries are shown in Fig. 4. Leakage flow through the annular seal thus forms a flow path that leads from the high-pressure discharge outlet back to the low-pressure suction side of the impeller.

The pump performance characteristics at the Best Efficiency Point (BEP) are stated in Table 6 from Van der Walt (2021), where $\eta P = \rho g H Q$ from Gülich (2014).

To calibrate the ROM model, the relevant test values were generated using the original Gülich model (Gülich, 2014). The calibrated ROM model was then verified by comparing the values predicted by the model with the corresponding results of the 1D fluid network simulation code Flownex (Flownex International, 2018), which has its own built-in model for an annular seal.

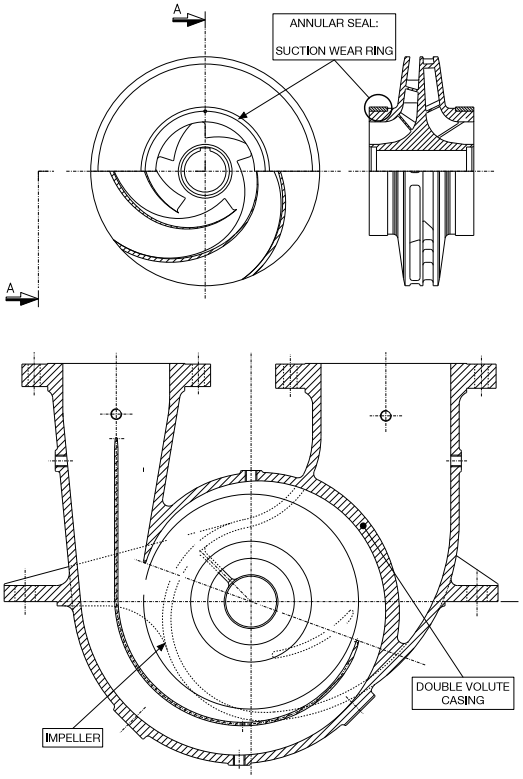

Fig. 3. Drawings depicting the subject pump's impeller and double volute layout showing location of suction wear ring (Van der Walt, 2021).

Table 6
Case study parameters obtained from original pump documentation and calculation (Van der Walt, 2021).

Parameters at best efficiency point (BEP)			
Variable	Value	Unit	Description
$NPSHR_{3\%}$	9	m	Net Positive Suction Head
Q	1150	m^3/h	Volumetric flow rate
H	286.55	m	Head delivered per pump stage
η	82.77	%	Operating efficiency
P	1084.8	kW	Electrical power
n	2985	RPM	Rotational speed of the impeller
d_{imp}	0.473	m	OD of the impeller

Table 7
Independent input variables for the subject pump in the case study (Van der Walt, 2021).

s	d_{sp}	n	L_{sp}	ζ_{EA}	ϵ
m	m	RPM	m	–	m
0.00025	0.2655	2985	0.0379	1.1787	0

4.2. Parameter set for calibration

In order to verify the selected mathematical model, it is calibrated and then tested against existing software. The inputs of the independent variables used for both the calibration and the verification are shown in Table 7. The parameters in Table 7 were taken from the operational values and dimensions of the physical pump used in the case study, documented by Van der Walt (2021).

IAPWS guidelines were used to update the properties of the fluid at every temperature point; density (ρ) was calculated using IAPWS R7-97 (2012) and dynamic viscosity (μ) was calculated using Huber et al. (2009). The kinematic viscosity, ν, was then calculated using the equation $\nu = \mu/\rho$ for each operating point. During property calculations, the inlet absolute pressure of the pump was used as the reference pressure,

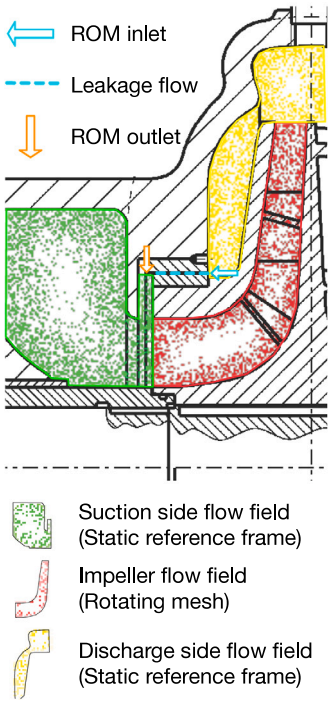

Fig. 4. Detailed cross section showing suction wear ring with leakage flow path and relevant flow field regions.

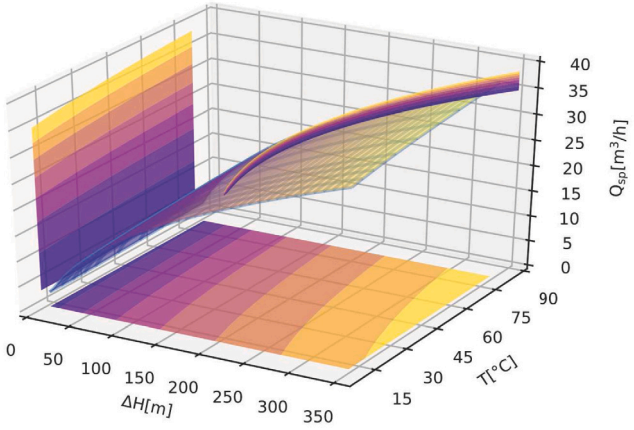

Fig. 5. Annular flow rate Q_{sp} as function of fluid temperature T and pressure differential ΔH across the annulus.

since the pressure increase due to the pumping mechanics will impact the fluid properties to an insignificant degree for an incompressible liquid.

The values were calculated in a pressure head range of $10\,m \leqslant \Delta H \leqslant 350\,m$ and a temperature range of $283.15\,K \leqslant T \leqslant 353.15\,K$. Values are shown in Fig. 5 with selected values listed in Table 8.

4.3. Gülich-Flownex verification

Table 7 specifies a surface roughness (ε) of 0 m; this is due to the fact that Flownex was unable to accommodate the surface roughness in its evaluation of rotating annular flow at the time of implementation. Thus, a base case of $\varepsilon = 0\,m$ was selected for verification.

According to Flownex International (2018), Flownex calculates the expected annular flow with an iterative process that combines the techniques outlined in the publications by Yamada (1962), Kaye and Elgar

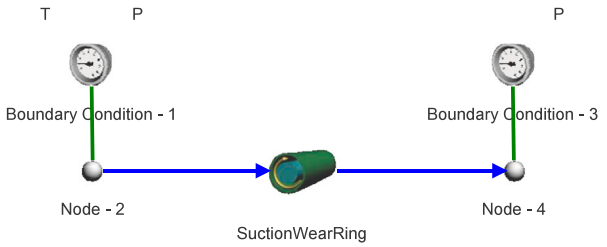

Fig. 6. Model created with network components in Flownex.

Table 8
Flow rates from Gülich model verified against Flownex.

ΔH [m]	T [°C]	Gülich Q_{sp} [m³/h]	Flownex Q_{sp} [m³/h]	Gülich/Flownex
45	10	9.516	9.363	1.0163
80	15	14.430	14.071	1.0255
105	20	17.408	16.967	1.0260
135	25	20.539	20.009	1.0265
180	30	24.583	23.989	1.0248
205	40	26.957	26.346	1.0232
225	50	28.827	28.224	1.0214
160	60	24.049	23.531	1.0220
135	70	22.058	21.586	1.0219
105	80	19.250	18.826	1.0225

Table 9
Analysis of G'ulich-Flownex comparison ratio: G'ulich/Flownex.

Data points	Average	Median	σ
680	1.0238	1.0242	0.0118

(1958), Cornish (1933) and Taylor (1923). These methods have been verified and validated and are described in the Flownex 8.9.1.3592 release documentation.

Fig. 6 shows the setup of the model in Flownex: An annular flow element ("SuctionWearRing") is connected to an inlet and an outlet node, where the appropriate temperature (T) and static pressure (p) boundaries are defined. Absolute static pressure values at the inlet and outlet nodes were specified with reference to the required differential head (ΔH) with the inlet T adapted as required for the specified test points. For flow rate calculations, the annular flow element was refined with 20 sub-elements to reach full convergence after each step. The working fluid was specified as clean water from the Flownex Fluid Library: "H2O - Water - General (Two Phase Fluids)".

Table 8 shows a (shortened) range of test points where the original values from the Gülich model are compared with the calculated flow rates Q_{sp} from Flownex. Modified units for Q_{sp} and T are used to facilitate the interpretation of the magnitudes compared to Fig. 5.

A summary of the comparison is presented in Table 9. Based on the evaluation of Table 9; the method proposed by Gülich generally predicts approximately 2.4% more leakage flow compared to the corresponding Flownex results when considering $\epsilon = 0\,\text{m}$.

The Gülich-Flownex comparison ratio (Gülich/Flownex) was analysed for 680 data points, resulting in an average ratio of 1.0238 with a median value of 1.0242 and a standard deviation of $\sigma = 0.0118$.

The Gülich model was therefore judged to be consistent over the stated ranges of temperature and differential head values and can be considered accurate and fit for purpose.

4.4. Gülich-ROM calibration and verification

A ROM was constructed using the method outlined in Sections 2 and 3 using the values generated by the Gülich model. The resulting equations that were obtained are shown in Eqs. (11a) to (11e).

$$d(\Delta H)T^3 + c(\Delta H)T^2 + b(\Delta H)T + a(\Delta H) = Q_{sp} \tag{11a}$$

Table 10
Flow rates from Gülich model compared with ROM.

ΔH [m]	T [°C]	Gülich Q_{sp} [m³/h]	ROM Q_{sp} [m³/h]	$\frac{\text{Gülich}}{\text{ROM}}$
45	10	9.516	9.465	1.0054
80	15	14.430	14.466	0.9975
105	20	17.408	17.441	0.9981
135	25	20.539	20.530	1.0004
180	30	24.583	24.552	1.0013
205	40	26.957	26.952	1.0002
225	50	28.827	28.845	0.9994
160	60	24.049	24.011	1.0016
135	70	22.058	22.045	1.0006
105	80	19.250	19.296	0.9976

Table 11
Analysis of values; Gülich/ROM.

Data points	Average	Median	σ
680	0.9986	1.0	0.0125

$$\begin{aligned} &1.17449\times10^{-11}\Delta H^5 - 1.31299\times10^{-8}\Delta H^4 + \cdots \\ &+ 5.83278\times10^{-6}\Delta H^3 - 1.36951\times10^{-3}\Delta H^2 + \cdots \\ &+ 0.246651\Delta H + 0.164876 = a(\Delta H) \end{aligned} \tag{11b}$$

$$\begin{aligned} &7.51733\times10^{-14}\Delta H^5 - 7.90636\times10^{-11}\Delta H^4 + \cdots \\ &+ 3.18534\times10^{-8}\Delta H^3 - 6.28108\times10^{-6}\Delta H^2 + \cdots \\ &+ 7.70495\Delta H\times10^{-4} + 0.029208 = b(\Delta H) \end{aligned} \tag{11c}$$

$$\begin{aligned} &- 6.43846\times10^{-16}\Delta H^5 + 6.81099\times10^{-13}\Delta H^4 - \cdots \\ &- 2.76039\times10^{-10}\Delta H^3 + 5.45809\times10^{-8}\Delta H^2 - \cdots \\ &- 6.56047\Delta H\times10^{-6} - 2.40868\times10^{-4} = c(\Delta H) \end{aligned} \tag{11d}$$

$$\begin{aligned} &2.34674\times10^{-18}\Delta H^5 - 2.50829\times10^{-15}\Delta H^4 + \cdots \\ &+ 1.02979\times10^{-12}\Delta H^3 - 2.06901\times10^{-10}\Delta H^2 + \cdots \\ &+ 2.53314\Delta H\times10^{-8} + 9.80977\times10^{-7} = d(\Delta H) \end{aligned} \tag{11e}$$

Independent variables were selected and specified across the same parameter ranges as defined in Section 4.2. A range of values was generated and a shortened version of this set is presented in Table 10 with modified units for Q_{sp} and T to facilitate the interpretation of the magnitude and comparison with Fig. 5.

A comparison between the corresponding values of Q_{sp} predicted by the ROM and Gülich models is given in Table 11. The Gülich-ROM comparison ratio (Gülich/ROM) was analysed for 680 data points, resulting in an average ratio of 0.9986 with a median value of 1.0 and a standard deviation of $\sigma = 0.0125$.

Upon evaluation of Table 11, the ROM generally predicted on average 0.14% less leakage flow with a 0% median deviation compared to the Gülich model when considering $\epsilon = 0\,\text{m}$. Therefore, the ROM can be judged as consistent and sufficiently accurate over the stated ranges of temperature and differential head values and can be considered suitable for use.

5. Implementation in Ansys CFX

The method described in Sections 2 to 4 can be implemented in any CFD software suite with user scripting capability. An example of such implementation for the determination of ΔH, T, and Q_{sp} is presented using Ansys CFX Expression Language (CEL).

Various key variables need to be calculated prior to implementing a ROM of the intended system, while other parameters are calculated and updated per iteration during simulation run-time. The methodology can be summarised by these three steps:

5.1. Extract boundary differential head and temperature from detailed 3D model

The values for ΔH and T are obtained from the detailed 3D simulation region by specifying the annular entrance and exit of the seal as named selection boundaries. The annulus entrance is located on the discharge volute and is named `REGION:Discharge_WearRing_Interface`; the annulus exit is located on the suction volute side and is named `REGION:Suction_WearRing_Interface`.

ΔH = `WearRingdeltaH` is calculated as:

```
(((areaAve(Pressure)
@ REGION:DischargeWearRing_Interface)
/(g*areaAve(density)
@ REGION:Discharge WearRing_Interface))-((
areaAve(Pressure)
@ REGION:Suction_WearRing_Interface)
/(g*areaAve(density)
@ REGION:Suction_WearRing_Interface)))/(1[m])
```

T=`WearRingInletTemperature` is calculated by:

```
((areaAve(T)
@REGION:Discharge WearRing_Interface
)/(1[K]))-273.15
```

5.2. Calculate leakage flow using the ROM model

After performing the required flow calculations using the results extracted from the named 3D selections, ΔH and T are passed as inputs to the ROM function that calculates Q_{sp}.

Q_{sp} = `WearRingLeakageROM` is calculated by:

```
(((ROMx3const*WearRingInletTemperature^3)+
(ROMx2const*WearRingInletTemperature^2)+
(ROMxconst*WearRingInletTemperature)+
(ROMcconst))/60/60)*(1[m^3/s])*
areaAve(density)
@REGION:Discharge WearRing_Interface
```

It should be noted that the equations for ΔH and T should be non-dimensionalised before the implementation of the constructed ROM. After the implementation of the method, the answer will be redimensionalised for input back into the main solver. Note that the unit of flow rate for the inlet boundary condition in the CFX solver is kg/s, and therefore Q_{sp} would require conversion to this unit. The noted variables `ROMx3const`, `ROMx2const`, `ROMxconst` and `ROMcconst` are respectively equal to $d(\Delta H)$, $c(\Delta H)$, $b(\Delta H)$ and $a(\Delta H)$.

5.3. Return leakage flow to the main simulation model

The calculated result from the ROM is the leakage flow Q_{sp}. This parameter is subsequently returned as the outlet flow rate to the `REGION:Discharge_WearRing_Interface` boundary on the discharge volute side and as the inlet flow rate to the `REGION:Suction_WearRing_Interface` on the suction side volute's named selection boundary.

6. Conclusion

The proposed ROM methodology was verified for accurate modelling of leakage flow in a centrifugal pump with a single-stage rotating annular seal with a hydraulically smooth surface finish and water as the working fluid.

The novel contributions of the study are the numerically robust modelling approach and the underlying theoretical principles (Section 2) that allow the analyst to account for the effects of surface roughness in the ROM model. The ROM methodology provides a framework where fluids, such as hydrocarbons, may also be used, as density and viscosity are included as parameters in the base theoretical model. However, care must be taken, when other fluids are used, to define loss coefficients in the base theoretical model in an appropriate manner, especially when dealing with high-viscosity cases or fluids with changing compositions.

The inclusion of surface roughness makes the proposed methodology superior to techniques focused on hydraulically smooth profiles due to the significant effect of roughness on leakage rate, Q_{sp}, while the ability to use other fluids gives wider applicability.

The paper also presents a method to implement the generated ROM in Ansys CFX Expression Language. The ROM has been validated as an embedded part of a fully detailed 3D transient centrifugal pump simulation (Van der Walt, 2021).

The future implementation of this ROM modelling approach by CFD analysts will ensure dramatic reductions in mesh size in annular flow regions, excellent solution accuracy, an increase in overall solver speed, and an improvement in convergence behaviour. With appropriate consideration, the methodology can be adapted for rotating annular seals of various designs and operating with water or alternative fluids, e.g. hydrocarbons. This makes it a valuable tool for geoenergy applications where enhancing and monitoring the energy efficiency of geothermal systems (in particular, turbomachinery components) are of importance.

Compressors, pumps, and turbines are vital components of underground gas storage, hydrogen production, and geothermal energy generation operations. By combining ROMs with advanced techniques (such as artificial intelligence, machine learning, and data analytics), predictive models can be developed that adapt quickly to changing operating conditions, ensuring the continued efficiency of geoenergy systems.

CRediT authorship contribution statement

Johannes Petrus van der Walt: Conceptualisation, Data curation, Formal analysis, Investigation, Methodology, Project administration, Resources, Software, Validation, Visualisation, Writing – original draft. **Jan-Hendrik Kruger:** Data curation, Software, Supervision, Writing – review & editing. **Charl Gabriël du Toit:** Supervision, Writing – review & editing.

Declaration of competing interest

The authors declare that they have no known competing financial interests or personal relationships that could have appeared to influence the work reported in this paper.

Data availability

No data was used for the research described in the article.

Declaration of Generative AI and AI-assisted technologies in the writing process

During the preparation of this work the author(s) used Writefull for Overleaf (www.writefull.com) in order to provide language feedback during revision. After using this tool/service, the author(s) reviewed and edited the content as needed and take(s) full responsibility for the content of the publication.

References

American Petroleum Institute, 2011. API STD 610: Centrifugal Pumps for Petroleum, Petrochemical and Natural Gas Industries. International Standard, (11th, Errata), American Petroleum Institute, Washington D.C., URL: https://global.ihs.com/doc_detail.cfm?&input_doc_number=&input_doc_title=&document_name=API%20STD%20610&item_s_key=00010651&item_key_date=880530&origin=DSSC.

Ansys, Inc., 2023. Ansys Engineering Simulation Software. ANSYS, Inc, URL: https://www.ansys.com/.

Bloch, H.P., 2011. Pump Wisdom: Problem Solving for Operators and Specialists. Wiley, Hoboken, N.J.

Bradie, B., 2006. A Friendly Introduction to Numerical Analysis. Pearson Prentice Hall, Upper Saddle River, New Jersey.

Cornish, R.J., 1933. Flow of water through fine clearances with relative motion of the boundaries. Proc. R. Soc. A Math. Phys. Eng. Sci. 140 (840), 227–240. http://dx.doi.org/10.1098/rspa.1933.0065.

Flownex International, 2018. Flownex Library Manual. Flownex International, URL: https://flownex.com.

Flownex International, 2023. Flownex Simulation Environment. Flownex International, URL: https://flownex.com.

Gülich, J.F., 2014. Centrifugal Pumps, third ed. Springer-Verlag, Berlin, http://dx.doi.org/10.1007/978-3-642-40114-5.

Huber, M.L., Perkins, R.A., Laesecke, A., Friend, D.G., Sengers, J.V., Assael, M.J., Metaxa, I.N., Vogel, E., Mareš, R., Miyagawa, K., 2009. New international formulation for the viscosity of H2O. J. Phys. Chem. Ref. Data 38 (2), 101–125. http://dx.doi.org/10.1063/1.3088050.

IAPWS R7-97, 2012. Revised Release on the IAPWS Industrial Formulation 1997 for the Thermodynamic Properties of Water and Steam. Technical Report, Industrial Formulation for Thermodynamic Properties of Water and Steam, p. 49.

Kaye, J., Elgar, E., 1958. Modes of adiabatic and diabatic fluid flow in an annulus with an inner rotating cylinder. Trans. ASME 80, 753–765. http://dx.doi.org/10.1115/1.4012502.

Krige, D.G., 1951. A statistical approach to some basic mine valuation problems on the Witwatersrand. J. Chem. Met. Min. Soc. South Afr. 52 (6), 119–139.

Liebner, T., Cowan, D., Bradshaw, S., 2016. The influence of impeller wear ring geometry on suction performance. In: Proceedings of the 32nd International Pump Users Symposium. Turbomachinery Laboratories, Texas AM Engineering Experiment Station, Houston, Texas, pp. 1–18. http://dx.doi.org/10.21423/R1NK5X.

Munson, B.R., Okiishi, T.H., Huebsch, W.W., Rothmayer, A.P., 2013. Fundamentals of Fluid Mechanics, seventh ed. John Wiley & Sons, Inc, Hoboken, NJ.

Páscoa, J.C., Silva, F.J., Pinheiro, J.S., Martins, D.J., 2010. Accuracy details in realistic CFD modeling of an industrial centrifugal pump in direct and reverse modes. J. Therm. Sci. 19 (6), 491–499. http://dx.doi.org/10.1007/s11630-010-0414-9.

Rennels, D.C., Hudson, H.M., 2012. Pipe Flow: A Practical and Comprehensive Guide. Wiley, Hoboken, N.J.

Taylor, G.I., 1923. Stability of a viscous liquid contained between two rotating cylinders. Phil. Trans. R. Soc. A 223 (605–615), 289–343. http://dx.doi.org/10.1098/rsta.1923.0008.

Van der Walt, J.P., 2021. Suction Recirculation Mitigation in a Double-Suction Centrifugal Pump (M.Eng. Dissertation). North-West University, Potchefstroom.

Volk, M., 2013. Pump Characteristics and Applications, third ed. CRC Press.

Yamada, Y., 1962. Resistance of a flow through an annulus with an inner rotating cylinder. Bull. JSME 5 (18), 302–310. http://dx.doi.org/10.1299/jsme1958.5.302.

Yedidiah, S., 1996. Centrifugal Pump User's Guidebook Problems and Solutions. Chapman & Hall, New York, NY.